ADVANCED MATERIALS
www.advmat.de

Recent Progress on Stability and Passivation of Black Phosphorus

Yohannes Abate, Deji Akinwande, Sampath Gamage, Han Wang, Michael Snure, Nirakar Poudel, and Stephen B. Cronin*

In memory of Mildred Dresselhaus.

From a fundamental science perspective, black phosphorus (BP) is a canonical example of a material that possesses fascinating surface and electronic properties. It has extraordinary in-plane anisotropic electrical, optical, and vibrational states, as well as a tunable band gap. However, instability of the surface due to chemical degradation in ambient conditions remains a major impediment to its prospective applications. Early studies were limited by the degradation of black phosphorous surfaces in air. Recently, several robust strategies have been developed to mitigate these issues, and these novel developments can potentially allow researchers to exploit the extraordinary properties of this material and devices made out of it. Here, the fundamental chemistry of BP degradation and the tremendous progress made to address this issue are extensively reviewed. Device performances of encapsulated BP are also compared with nonencapsulated BP. In addition, BP possesses sensitive anisotropic photophysical surface properties such as excitons, surface plasmons/phonons, and topologically protected and Dirac semi-metallic surface states. Ambient degradation as well as any passivation method used to protect the surface could affect the intrinsic surface properties of BP. These properties and the extent of their modifications by both the degradation and passivation are reviewed.

1. Introduction

Phosphorus is one of the most abundant elements with several allotropes, out of which white and red phosphorus are the most commonly available species.[1,2] Black phosphorus (BP) has been widely and successfully synthesized in bulk form for more than 100 years through high temperature and pressure conversion from the more common white or red phosphorus allotropes.[3] While the high temperature and pressure conversion process can produce crystalline samples with large sized grains, it also requires pressure greater than 10 kbar and temperature greater than 600 °C, which are inaccessible using common crystal growth techniques.[4] More recently, an alternative low-pressure vapor approach capable of producing millimeter sized crystals using mineralizer promoted short way vapor transport has been demonstrated.[5] These bulk growth methods have made it possible to synthesize material that is suitable for exfoliation of mono to many-layer BP flakes commonly used to fabricate optoelectronic devices and study their properties. For comprehensive details on synthesis of bulk BP, we encourage readers to refer to refs. [2] and [6]. Unlike bulk BP, which has been thoroughly studied, BP thin films have yet to be comprehensively investigated. Reviews of recent advances in synthesis, characterization and applications of BP thin films include refs. [7–10]. One of the first demonstrations was deposition of few nanometer thick BP films over 4 cm × 4 cm substrates by pulsed laser deposition; however, these films were found to be amorphous.[11] Thicker crystalline BP films were recently produced through a high temperature and pressure conversion of red phosphorus films on substrates up to 4 mm in diameter.[12] Using this approach, it may be possible to produce films with relatively higher crystal quality similar to ref. [4], but the crystal growth may be limited to small areas. Blue phosphorus, which has a honeycomb structure similar to graphene, has been produced by molecular beam epitaxy (MBE) on metal substrates recently. Formation of small monolayer islands of blue phosphorus stabilized on Au(111) and Te covered Au(111) surfaces using MBE demonstrates a route toward producing 2D phosphorus films.[13]

Prof. Y. Abate
Department of Physics and Astronomy
University of Georgia
Athens, GA 30602, USA
E-mail: yabate@physast.uga.edu
Prof. D. Akinwande
Department of Electrical and Computer Engineering
University of Texas at Austin
Austin, TX 78758, USA
Dr. S. Gamage
Department of Physics and Astronomy
Georgia State University
Atlanta, GA 30303, USA
Prof. H. Wang, N. Poudel, Prof. S. B. Cronin
Viterbi School of Engineering University of Southern California
Los Angeles, CA 90089, USA
Dr. M. Snure
Air Force Research Laboratory
Wright Patterson Air Force Base
OH 45433, USA

DOI: 10.1002/adma.201704749

The interest in BP exploded recently when it was realized that BP belongs to the family of materials that can also be exfoliated. Furthermore, BP possesses several interesting physical properties with unique potential applications in optoelectronics. BP has strong in-plane anisotropy, which stems from its orthorhombic crystal structure with space group *Cmca*. It forms a puckered honeycomb network where the in-plane x and y axes correspond to orientation of atoms in armchair (AC) and zigzag (ZZ) directions, respectively. This orientation results in two independent in-plane components of the dielectric tensor that are different from each other, which opens a platform to manipulate anisotropic interactions of light with BP and electrical conductance.[14] **Figure 1**a shows the schematic lattice structure of black phosphorus with the AC and ZZ crystal directions indicated. The band structures for 1-layer, 2-layer, and 3-layer BP as calculated by density functional theory (DFT) simulation are also presented in Figure 1b. The band gap in black phosphorus increases with decreasing layer number due to the 2D confinement of carriers. An important consequence of strong Coulomb interactions in 2D layered semiconductors is the formation of tightly bound neutral or charged excitons.[15–17] The photophysics of the 2D systems are dominated by the transitions of these excitons. As a result, layered and 2D materials offer an excellent platform to explore exciton physics as well as engineer practical devices for novel applications.[18,19] In addition, the close proximity of external stimuli to the exciton wave function can offer unprecedented tunability and interaction with photons and polaritons.[20] Excitonic effects play a major role in the optical transitions of BP and unlike other layered materials, excitons in BP display the expected in-plane anisotropy. BP also offers unprecedented capability to manipulate propagating polaritons (plasmons or phonons) due to its anisotropic property. BP exhibits striking anisotropic quasiparticle properties and many-body interaction effects that offer an exciting hunting ground for new physics. Semiconductor to Dirac semimetal or semiconductor to topological quantum-phase transitions that accompany gap modifications in mono and multilayer BP give rise to exotic quasiparticles with unique physical properties, which have been explored recently both experimentally and theoretically.[1]

In addition to providing a unique platform for novel fundamental science explorations, BP is an immensely promising material for flexible optoelectronic applications. Although bulk BP was discovered over a hundred years ago, it was not until 2014 that field-effect transistors (FETs) with mono and multilayer BP as their channel material were demonstrated.[21–23] The typical thin film BP (≈4–10 nm thick) transistors show transfer characteristics with on/off current ratio in the range of 10^3–10^5 depending on the thickness of the BP channel. The devices also display decent saturation characteristics in their output current. Both these characteristics make it possible to develop BP transistors for digital logic applications in thin-film electronics as well as flexible electronic systems, which stands in contrast to devices based on other high mobility layered materials such as graphene. Graphene transistors typically show relatively lower on/off ratios and a signature lack of current saturation in its output characteristics, both resulting from the zero band gap nature of the material. Moreover, BP's typical on–off current ratio and current saturation characteristics also offer the prospects for integrating BP-based optical devices with electronic read-out circuitry that can be constructed on the same material. Furthermore, the high hole mobility in a few layered black phosphorus makes the material advantageous over commercial Si, which has hole mobility around 450 $cm^2\ V^{-1}\ s^{-1}$, for making p-channel transistors.[24] BP offers an alternative material for high hole mobility semiconductors like Ge. The mobility for both electrons and holes in BP is also high making it suitable for thin film and flexible electronic applications. Bulk BP features a narrow band gap of 0.3 eV, which is attractive for reducing the operating voltage

Yohannes Abate is an Associate Professor at the Department of Physics and Astronomy, the University of Georgia. He received his Ph.D. in physics from the University of Iowa in 2006. During 2006–2009, he was a postdoctoral research fellow at the University of California, Berkeley and Lawrence Berkeley National Laboratory. His research in nano-optics includes low-dimensional materials, strongly correlated systems and recently enveloped viruses.

Sampath Gamage received his B.Sc. degree in physics from the University of Colombo, Sri Lanka. He obtained his Ph.D. in nano-optics under the supervision of Prof. Yohannes Abate from Georgia State University, Georgia, USA in summer, 2017. His research interests include studying the optical properties of layered materials and growth and characterization of semiconductor thin films.

Stephen B. Cronin is an Associate Professor and the Gordon S. Marshall Early Career Chair in Engineering at the University of Southern California. He received his Ph.D. in physics at MIT in 2002. He subsequently conducted his post-doctoral research at Harvard University. He studies optoelectronics, thermal and thermoelectric transport, and photocatalysis in a variety of nanoscale materials and devices.

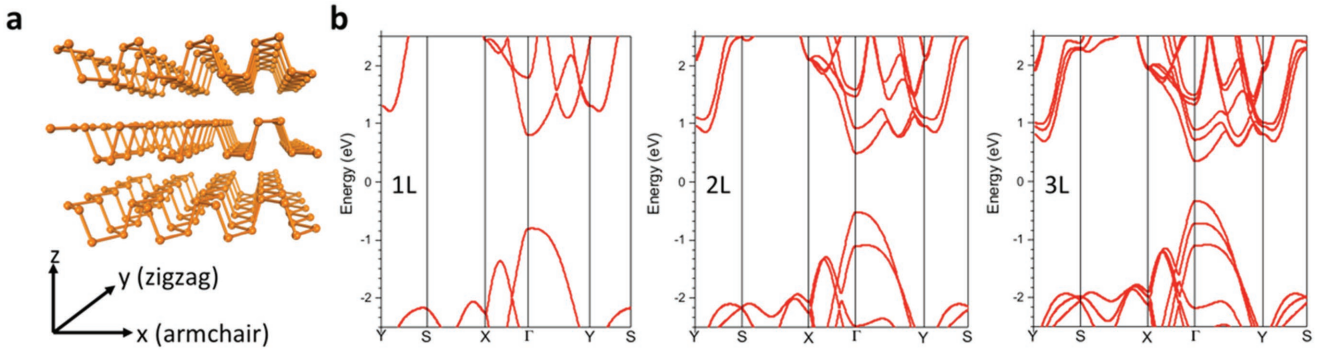

Figure 1. Lattice cartoon structure of BP with the armchair and zigzag crystal directions (a), and theoretical DFT band structure calculations for 1-layer, 2-layer, and 3-layer of BP (b) showing decreasing band gap with increasing layer number due to the 2D confinement of carriers.

and power consumption in logic devices. Moreover, the on/off current ratio and mobility of BP transistors have been observed to be strongly dependent on the thickness of the thin film BP channel. Typically, the on/off current ratio of a BP device rises as the film thickness decreases, which is a result of the charge screening effect. Li et al. estimated the screening length in BP devices to be ≈2.9 nm.[25] By assuming a different carrier density, Low et al.[25,26] predicted the screening length in BP thin film to be ≈10 nm. Though thinner BP channel can, in principle, lead to higher on/off current ratio, it can also be more susceptible to degradation by oxidation. Thinner BP samples are also easily affected by charge impurities in the surface and substrate environment, resulting in scattering centers that can significantly reduce the carrier mobility. Researchers have also been endeavoring to demonstrate field effect devices based on single-atomic layer black phosphorus that demonstrate the ultimate electrostatic control by the gate over the channel and relatively higher mobility due to 2D quantum confinement. Such efforts, however, have only resulted in very limited progress due to the formidable challenge of preserving single-layer BP from oxidation.

Achievement of all the exciting fundamental scientific and technological promises of BP depends on finding innovative solutions to protect BP from degradation under an ambient environment. Although most van der Waals (vdW) materials that can be exfoliated are not entirely air stable, the extent of ambient degradation is comparatively quite severe in BP. Single-layer BP (phosphorene) exfoliated in ambient degrades completely in a matter of hours making it impossible to expose phosphorene to air.[27] Few-atoms thick BP also degrades in air in a matter of days. This lack of stability under ambient conditions severely undermines the usability of mono and multi-layered BP and indirectly determines the practicality and cost of any future devices that could be provided by this material. In the first review article written on BP, just after its revival as a member of vdW family of materials, Dresselhaus and co-workers urged the community that the ambient degradation of BP should not discourage researchers and device engineers from attempting to exploit the full potential that this material offers in creating novel technology and pushing the limit of scientific understanding. The authors mention that, "Learning from the commercial success of relatively unstable materials like organic semiconductors and the technological importance of many toxic and potentially unstable materials like mercury cadmium telluride (MCT), we believe that the stability issue should not be viewed as a showstopper preventing further research on this material. It is most likely that good passivation and packaging technology can resolve this issue."[1] We can confidently say that this time has arrived. Over the last 2–3 years, the scientific community has put forth an enormous effort in order to understand the degradation problem in BP and mitigate the instability issues using many innovative approaches. In this review, we attempt to reexamine the degradation topic based on recent advances and highlight some of the most optimistic progress particularly related to passivation issues.

2. Stability and Passivation

Layered materials are susceptible to degradation when exposed to an ambient environment due to enhanced chemical reactivity of their extraordinarily high surface areas.[28] BP suffers from degradation within a few days of exposure to ambient conditions.[29,30] Although bulk BP degradation was observed early on by Yau et al. while performing scanning tunneling microscopy surface imaging experiments,[31] it is only recently that various groups (Castellanos-Gomez et al.[32] and Wood et al.[30] were the earliest two) examined how exfoliated BP degrades in ambient environments through a comprehensive set of microscopy and spectroscopy techniques. The effects of degradation are commonly seen as the formation of liquid droplets on the surface of a BP flake, using atomic force microscopy (AFM) or optical microscopy. These degradation processes were extensively studied by Gamage et al. using nanoscale time series imaging over several months as shown in **Figure 2**.[29] The degradation begins after ambient exposure as small bubbles start to form. The rate of increase in area and volume of these bubbles is slower in the beginning of the degradation process but then the rate of growth in bubble size increases rapidly (approximately exponentially) before reaching saturation, producing an S-shaped growth curve (sigmoid growth curve).[29] Oxidation effects have been thoroughly analyzed using Raman spectroscopy showing a systematic and continuous degradation of BP's Raman (A^1_g = 335 cm^{-1}, B_{2g} = 434 cm^{-1}, and A^2_g = 460 cm^{-1}) signature as crystalline layers become oxidized (**Figure 3**). Since

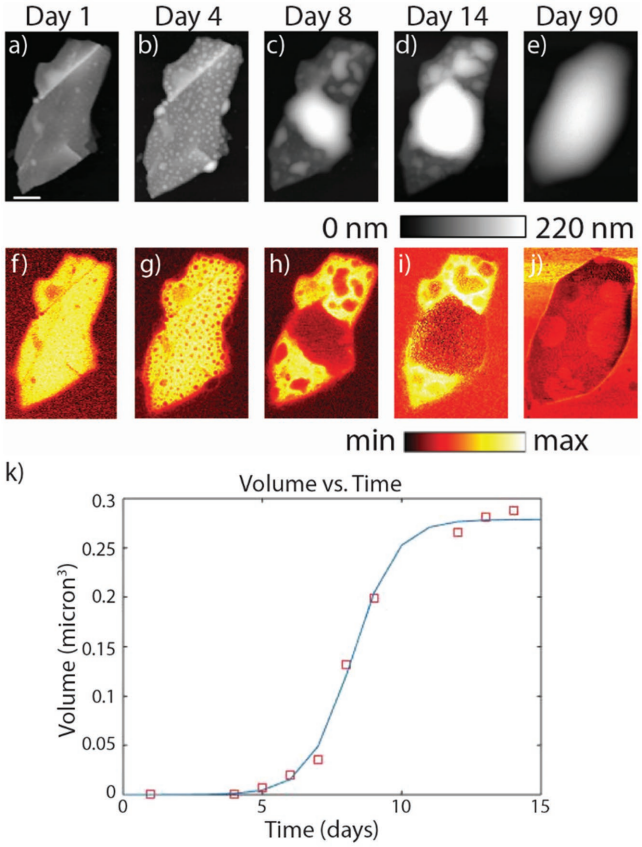

Figure 2. Time evolution of: a–e) topography and f–j) near-field third harmonic optical amplitude taken at a laser wavelength of = 10.5 µm of freshly exfoliated unencapsulated BP with thickness 27 nm. Scale bar = 500 nm. k) Experimental (squares) and simulated (solid lines) results of volume of a degraded bubble. Reproduced with permission.[29] Copyright 2016, Wiley-VCH.

the oxidized layers do not contribute to the Raman signal, a significant decrease in peak intensities is observed with minimal shift in peak positions or full width at half maximum.[33,34] Favron et al. showed that the intensity ratio of the A^1_g/A^2_g modes could be an effective tool for detecting degradation.[35] Abellán et al. confirmed this finding later, observing an exponential decay in A^1_g/A^2_g with air exposure time, for flakes less than ≈10 nm thick.[36] Favron et al. investigated the light-induced oxidation of different layered black phosphorous.[35] They observed that the oxidation process is significantly delayed in the absence of light exposure. They also report that the photo-oxidation takes longer for thicker part of the flakes (more than six layers) than the thinner flakes and the oxidation rate is directly proportional to light intensity.

Significant progress has been made both experimentally and theoretically to understand the exact mechanism of BP degradation in air. BP's susceptibility to degradation has been related to its unstable bonding structure arising from the free electron lone pairs of phosphorus atoms.[30,37] Studies employing in situ Raman (Figure 3), transmission electron microscopy and modeling have established that the rate of oxidation of BP depends on oxygen concentration, light intensity, and energy gap.[35] Luo et al. have systematically investigated the kinetics of BP oxidation under controlled oxidative environment consisting of different ratio of O_2 and H_2O employing X-ray photoelectron spectroscopy.[38] They concluded that BP oxidation is likely to be caused by a synergetic effect of water and oxygen where water drives the oxidation via the reaction with the surface oxide which then creates oxygen dissociations. Theoretical calculations have also predicted a three-step degradation mechanism: a generation of superoxide under light, dissociation of the superoxide, followed by dissociation after reaction with water.[39] In addition, a number of earlier works on BP oxidation in air support the combined role of O_2 and H_2O.[32,40,41] In contrast, recent works have shown that BP is stable in deoxygenated H_2O[31] and can also be used as an effective recoverable humidity sensor if isolated from light and/or O_2.[33] Water has also been shown to play an important role in stabilizing BP after solution exfoliation.[42] By using DFT to study BP oxidation, Ziletti et al. showed that O_2 will strongly chemisorb to the surface and can result in the formation P—O bonds without the presence of H_2O.[43] Instead H_2O is only weakly physisorbed to the BP surface. A combination of DFT and first principles molecular dynamics calculations also found that O_2 will spontaneously dissociate on phosphorene at room temperature and that H_2O does not interact directly with the pristine phosphorene.[44] In fact, pristine BP is hydrophobic and it is only after the oxidation process to form PO_x that the surface becomes hydrophilic.[45] This degradation is also highly thickness dependent. Single-layer BP (phosphorene) is the fastest to degrade (within minutes after exfoliation).[35]

2.1. Passivation Techniques

Various techniques have been proposed and tested for effective passivation of BP via surface functionalization or coatings, including organic covalent functionalization and inorganic and hybrid organic–inorganic coatings. Coating can serve as a physical barrier preventing oxygen from reaching the surface. The coating can also bind to BP's lone pair of electrons preventing the oxidation reaction. Reported passivation approaches, coating, and characterization methods are summarized in **Table 1** and examples of different passivation approaches are shown in **Figure 4**.

2.1.1. Organic Functionalization of BP

Keeping the lone pair electrons in BP paired by reacting them with ligands other than oxygen has been shown to be an effective way to enhance the stability of BP in water and air. Hersam's group reported effective suppression of the chemical degradation of BP by covalent aryl diazonium functionalization.[46] Zhao and co-workers used titanium sulfonate (TiL_4) ligand for surface coordination of BP and formed TiL_4-coordinated BP that showed enhanced surface stability when exposed to water or humid air.[47] Polymers have also been proposed as alternative ligands for surface coordination of BP.[48] Improved stabilization of BP against oxidation was also demonstrated by noncovalent functionalization of BP with 7,7,8,8-tetracyano-p-quinodimethane (TCNQ) and a perylene bisimide.[49]

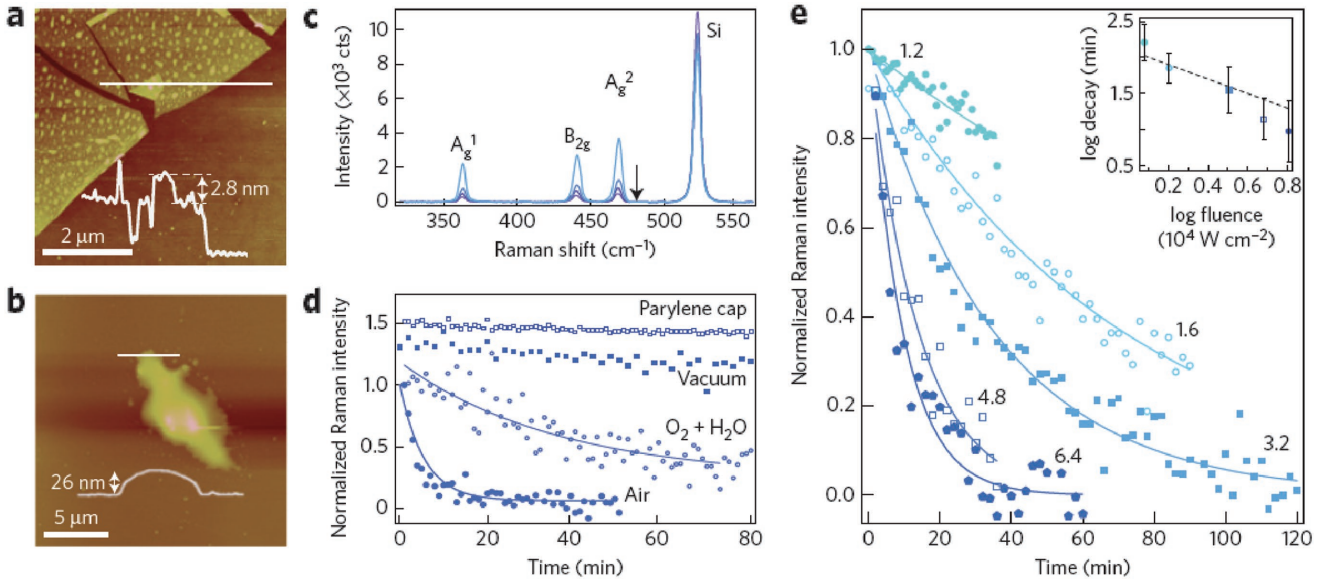

Figure 3. Photo-oxidation of multilayer 2D phosphane under constant illumination at room temperature. a,b) AFM images taken immediately after exfoliation and a few days later under ambient conditions. c) Raman spectra on a 5 nm thick sample measured in air. d) Time dependence of the integrated intensity of the Ag^2 Raman mode in different conditions: air, vacuum, mixture of O_2 and H_2O, and in air encapsulated under a 300 nm layer of parylene cap. e) Time evolution of the integrated Raman intensity of the Ag^2 mode at different laser fluences. Experiments in (c)–(e) are made with constant laser illumination and curves in (d) and (e) are monoexponential fits to the data (solid lines). Reproduced with permission.[35] Copyright 2015, Nature Publishing Group.

2.1.2. Inorganic Coatings

Using atomic layer deposited (ALD) Al_2O_3 protective layers, Pei et al. controllably produced air-stable few to monolayer BP made using layer-by-layer thinning by O_2 plasma etching.[27] This process sputters P_xO_y species away from the top surfaces by colliding with oxygen plasma. Stable BP with high mobilities and on–off ratios was also demonstrated by encapsulating atomically thin BP between boron nitride (BN) layers followed by annealing at high temperatures.[50] Hybrid Al_2O_3/BN

Table 1. Effective passivation methods of BP. The monitored time indicated only refers to the duration BP is monitored and not the maximum time it stays stable.

Passivation technique	Time monitored	Coating method	Characterization technique	Ref.
Double layer capping of Al_2O_3 and hydrophobic fluoropolymer	30 d	ALD (Al2O3), spin-casting (fluoropolymer)	AFM, microwave impedance microscopy	[55]
BN-BP-BN heterostructure followed by annealing at 500 °C	≈7 d	Transfer technique	Charge transport measurements	[50]
Primarily of phosphorus pentoxide (P_2O_5)	2 d atmosphere exposure		Synchrotron-based photoelectron spectroscopy	[52]
Covalent aryl diazonium functionalization	≈10 d	Chemical functionalization	X-ray PES (XPS), Raman, AFM, charge transport, DFT calculations	[46]
Layer-by-layer thinning of BP by O_2 plasma, followed by Al_2O_3 coating	30 d	O_2 plasma etching and ALD (Al_2O_3)	Phase-shifting interferometry, photoluminescence spectroscopy, Raman spectroscopy	[27]
Thin film (10 nm or thicker) Al_2O_3 coating	90 d	ALD	s-SNOM, AFM	[29]
Ionophore coating	30 d	Spin coating	AFM, Raman, semiconductor parameter analyzer	[53]
Covalent functionalization with titanium sulfonate ligand	24 h (humid air)	Solution phase reaction	HR-TE, optical microscopy, AFM, HRXPS, Raman	[47]
7,7,8,8-tetracyano-p-quinodimethane (TCNQ) and a perylene bisimide	2 d (ambient)	Chemical approach	AFM, Raman, STEM-EELS	[49]
Liquid phase exfoliation in *N*-cyclohexyl-2-pyrrolidone (CHP)	11 d	Liquid phase exfoliation	AFM, Optical extinction and absorbance, TEM/ HRTEM, STEM	[56]
Al_2O_3 encapsulation	8 months	ALD	Charge transport	[104]
Hybrid Al_2O_3/BN encapsulation	6 months	BN transfer, ALD Al_2O_3	s-SNOM, charge transport	[51]

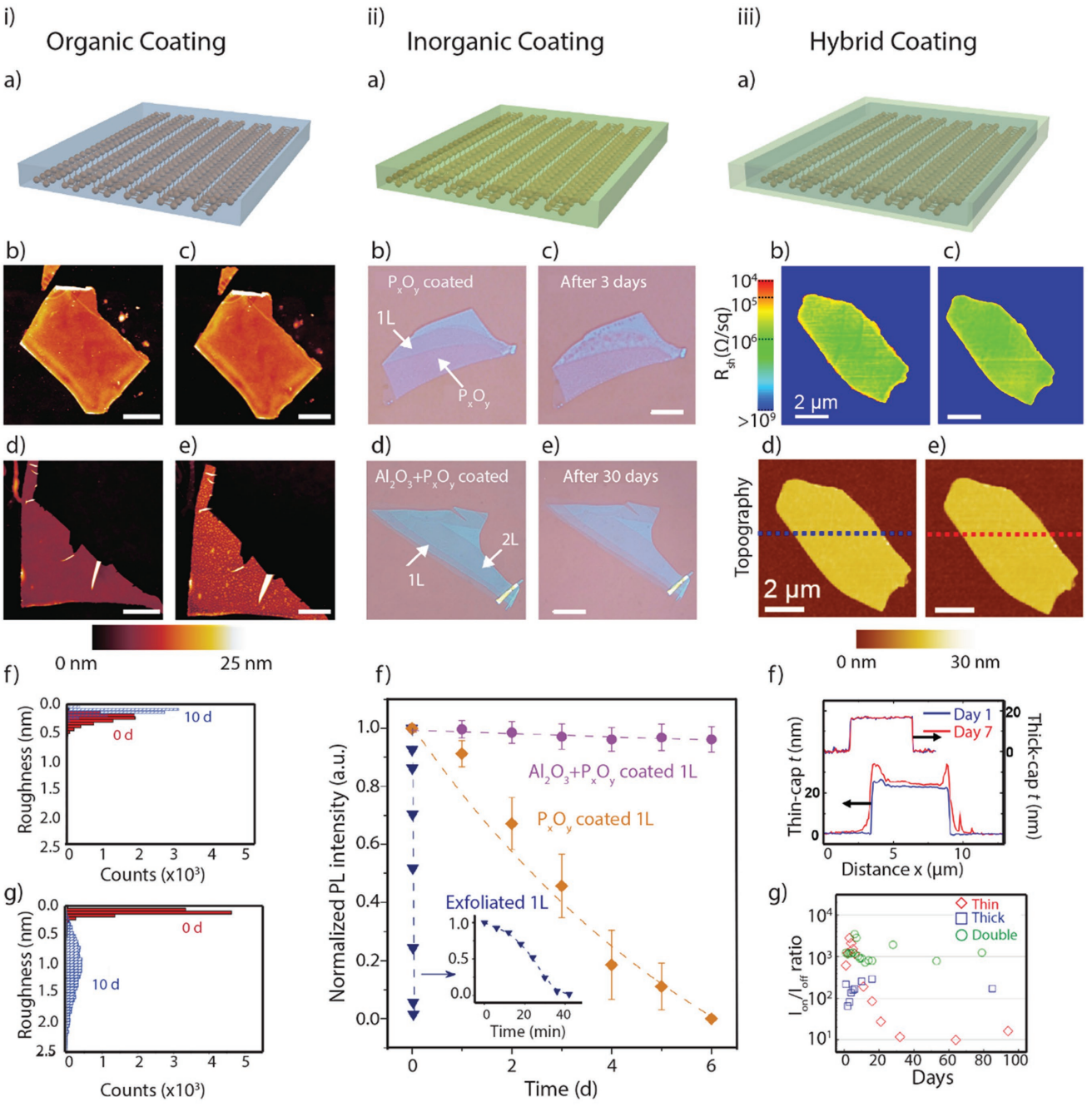

Figure 4. Surface passivation of BP by organic covalent functionalization (i), inorganic (ii), and hybrid organic–inorganic (iii) coatings. i: b–e) Reproduced with permission.[46] Copyright 2016, Nature Publishing Group. ii: b–f) Reproduced with permission.[27] Copyright 2016, Nature Publishing Group. iii: b–g) Reproduced with permission.[55] Copyright 2015, Nature Publishing Group.

layers have shown to significantly improve surface stability while enabling excellent FET device performance.[51] Using synchrotron-based photoelectron spectroscopy, it was also shown that P_2O_5 forms at the surface of BP and acts as a passivation layer for few days.[52] By coating BP with ionophore, Li et al. have demonstrated an air stable BP sensor that can detect multiple ions with high sensitivity better than graphene-based sensors.[53] Effective passivation of BP was also achieved via binding its lone pair of electrons to a titanium sulfonate ligand.[47]

2.1.3. Combination of Organic and Inorganic Coating

Kim et al. demonstrated that air-stable BP devices can be produced by a double-layer capping of Al_2O_3 and hydrophobic

fluoropolymer using microscopy, spectroscopy, and transport techniques.[54,55]

2.1.4. Liquid Exfoliation

It has been demonstrated that BP synthesized in large quantities by liquid phase exfoliation under ambient conditions in solvents such as *N*-cyclohexyl-2-pyrrolidone (CHP) is more stable than mechanically exfoliated few-layer BP. The enhanced stability in CHP is attributed to the fact that solvation shell protects the nanosheets from reacting with water or oxygen.[56]

3. Long-Term Stable and Reliable Devices

Degradation limits the performance of BP devices fabricated under ambient conditions. Degradation of BP results in the formation of a thin layer of insulating oxide that causes increased contact resistance.[57] Degradation also results in significant physical changes including nonuniform areal and volumetric expansion, which causes increased surface roughness and thus impacts carrier mobility.[58] Oxygen defects produce deep donor and/or acceptor levels in the band gap and form unnecessary complex defects. Koenig et al. observed significant *I*–*V* hysteresis characteristics that depend on the gate sweep direction much higher than that observed in graphene and other 2D crystals.[57] BP degradation alters its electrical properties and deteriorates FET performance by increasing threshold voltage, and decreasing on/off ratio and mobility.[30] Passivants can also modify performance. For example, passivants for MCT photoconductive detectors give rise to positive fixed charges, which alter performance of these photoconductive detectors.[59] Density functional theory studies have also found that absorption of transition metals on single-layer phosphorene could hinder use of this material for spintronics applications.[60] On the other hand, performance and applicability of BP can be enhanced by addition of Cu adatoms to lower the threshold voltage for n-type conduction without degrading the transport properties.[61] Adsorbed Ag^+ ions have been shown to interact with the conjugated π bonds improving BP stability.[62] The Ag^+ can bind lone electrons more strongly than O preventing oxidation. DFT computations have also predicted that doping phosphorene by organic molecules adsorbed on the surface noncovalently can significantly narrow its band gap.[63] High boiling point liquids, adsorbed on the surface, including water, can offer a facile method for improving stability that can be used for short term, like transporting samples, or/and long term between multiple processing or characterization steps.[56,64] Compared to solid passivation approaches, liquids are relatively easy to remove. Moreover, tight packing of these solvent molecules can efficiently impede penetration of oxygen molecules to the surface of BP. Ionic liquids are also promising candidates for both passivation and electrostatic gating. Abellán et al. used ionic liquids to stabilize flakes <10 nm thick for up to a week (**Figure 5**).[36]

Several approaches have been developed to address the stability of BP FETs. Wood et al. demonstrated that atomic layer deposited AlO_x overlayers effectively suppress ambient degradation, allowing encapsulated multi-layered BP FET to maintain high on/off ratios of $\approx 10^3$ and mobilities of ≈ 100 cm^2 V^{-1} s^{-1} for more than 2 weeks in ambient conditions.[30] Avsar et al. used graphene-*h*BN van der Walls structures to encapsulate the underlying black phosphorus (varying layers of 2 and 6) FET device in an inert argon environment.[65] They compared the transistor performance of exposed BP FETs with encapsulated BP FETs and observed that the nonencapsulated devices exhibited a hysteresis of ≈30 V in vacuum conditions while the encapsulated devices had hysteresis-free transport properties.[65] In their work, graphene was used as electrodes underneath the BP, and the mobility was reported as 63 cm^2 V^{-1} s^{-1} at room temperature.[65] Their devices demonstrated a 10% decrease in mobility when cooling down to a temperature of 100 K and a 30% decrease in mobility at a temperature of 10 K.[65] They showed that their device exhibited negligible hysteresis even after 2 months.[65] Chen et al. reported the fabrication of stable van der Waals heterostructure consisting of a few layers of black phosphorus sandwiched between two *h*BN layers to achieve field effect mobilities of almost 1350 cm V^{-1} s^{-1} at room temperature and on/off ratio of 10^5.[50] They attributed the high mobility for their BN–BP–BN devices to transport along the *X*-direction as opposed to the *Y*-direction, which was confirmed through polarization angle dependent Raman spectroscopy.[50] The mobility along the *X*-direction can be two times larger than that in the *Y*-direction.[21,50,66] The large on–off ratio and negligible hysteresis is attributed to the ultraclean BN–BP interfaces as well as high-temperature annealing (300–500 °C) of the encapsulated BP.[50] Cao et al. encapsulated their BP-based transistors between mono and sometimes bilayer *h*BN on top of Si/SiO_2 wafer.[54] They report a mobility of more than 4000 cm^2 V^{-1} for thicker (more than ten layers) devices, ≈1, 8, and 1200 for mono, bi, and tri-layer devices at cryogenic temperatures. Moreover, they noticed that there was no deterioration in the device quality even after several months. Chen et al. also demonstrated that the FET properties of their encapsulated samples show no degradation even after exposure to 60% humidity.[50]

Doganov et al. fabricated device structures that allowed them to directly compare the encapsulated and nonencapsulated parts of the same ultrathin black phosphorus flake.[40] For the BN-encapsulated part of the BP devices, they obtained an electron mobility of 62 cm^2 V^{-1} s^{-1} and, in the exposed region, the electron mobility was reported to be 5 cm^2 V^{-1} s^{-1} at 200 K.[40] To further improve upon BN encapsulated device performance, Yang et al. used a two-layer Al_2O_3/BN layer fabricated in an inert environment to produce ultraclean interfaces protected by the BN.[67] This hybrid Al_2O_3/BN layer improves stability and has resulted in FETs with a few-layer BP channel with record high on-currents and transconductance. Ryder et al. demonstrated that covalent functionalization of a few-layer black phosphorus using aryl diazonium can suppress the chemical degradation of BP devices even 3 weeks after ambient exposure through the formation of a carbon–phosphorus bond.[46] Zhao et al. used DFT calculations and molecular dynamics simulations to investigate the self-assembly of perylene-3,4,9,10-tetracarboxyluc dianhyrdride monolayers as a possible effective passivation layer.[68] SiO_2 passivation has also been used to prevent degradation of few-layer BP and maintain carrier mobility up to 500 cm^2 V^{-1} s^{-1}.[69] Kim et al. used graphene as a passivation

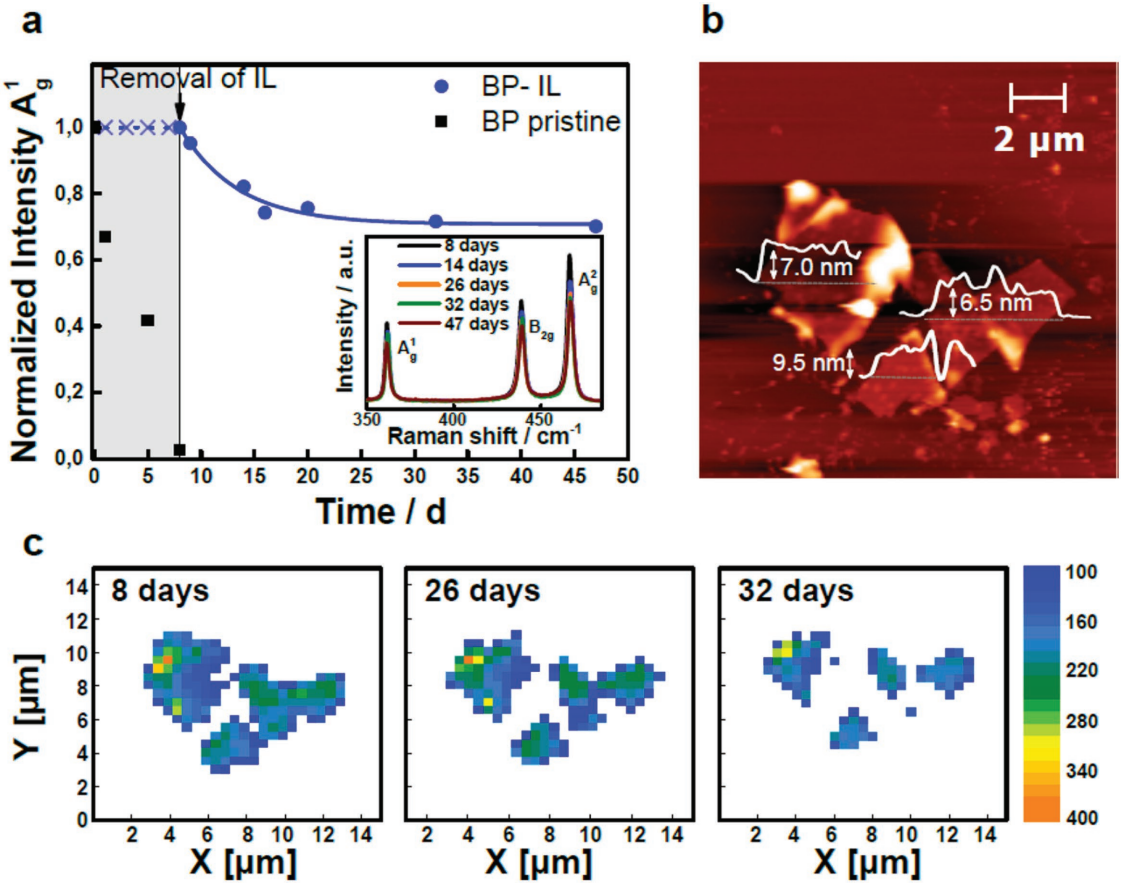

Figure 5. Surface passivation of BP using an ionic liquid (IL). a) Change in A^1_g mode intensity with time for flakes with and without IL passivation. b) AFM images of flake after IL removal. c) Scanning Raman map of a 6–10 nm thick BP flake over time the A^1_g color scale plots A^1_g intensity. Reproduced with permission.[36] Copyright 2017, American Chemical Society.

layer and performed Raman spectroscopy to demonstrate that the Raman peaks remain unchanged up to 4 d, after which the signal reduced to 90% of its original strength.[70] Black phosphorus has also been demonstrated as a promising material for flexible electronics. Zhu et al. realized flexible Al_2O_3 encapsulated BP devices on polyamide substrates with device mobilities of 310 cm^2 V^{-1} s^{-1}, which is five times more than the highest reported mobility values for other flexible transistors based on transition metal dichalcogenides.[71–74] Li et al. developed a BP sensor encapsulated with ionophore to demonstrate an air stable BP sensor.[53] The ionophore-encapsulated devices demonstrated no obvious degradation in their optical images (no bubbles and color change) for 30 d.[53] Their devices showed source–drain current, I_{ds} ($V_{ds} = -2.5$ V and V_{gs} varied from −5 to 10 V), variation of less than 10% after 1 week of exposure to ambient conditions, showing good stability.[53]

In the field of high-speed electronics, the high mobility of BP makes it possible to develop transistor devices that can operate at a frequency well into the gigahertz range for applications in thin film radio frequency (RF) electronics. The first BP RF transistors operating in the gigahertz frequency range were independently demonstrated by two research groups in late 2014. The device demonstrated by Wang et al. was fabricated along the *x*-direction of the BP crystal to take advantage of the highest possible carrier mobility.[75] With a channel length of 300 nm, the BP FETs were reported to show a short-circuit current gain cut-off frequency (f_T)of 12 GHz. The device also shows a maximum oscillation frequency (f_{max}) of 20 GHz as extracted from the frequency dependence of its unilateral gain. Compared to high-speed transistors based on graphene, BP transistors are more promising for achieving better power gain, which is an important parameter for applications in amplifiers, as indicated by its higher f_{max} than f_T. This is a direct result of the enhanced current saturation in BP devices due to BP's semiconducting nature as compared to graphene's semi-metallic nature. We believe that the high-speed performance of BP transistors still have plenty of room for improvement. Recent studies have shown that when BP is encapsulated between *h*BN, the mobility of the BP thin film can exceed 1000 cm^2 V^{-1} s^{-1} at room temperature and be above 6000 cm^2 V^{-1} s^{-1} at low temperatures. Based on the continuous advancements in the quality of contacts, the device fabrication process, and the progressive scaling of channel length, it is reasonable to expect that the frequency performance of BP transistors might be able to exceed the 100 GHz in the near future.

A unique feature that BP devices offer for RF applications is the ease with which ambipolar conduction characteristics can be achieved in these devices. With a moderate level of electrostatic bias, the Fermi level in BP can be readily shifted across

its narrow band gap and the channel conduction can be modulated by the gate bias between p-type and n-type conductions. Such ambipolar channel properties and relatively symmetrical transfer characteristics between electron and hole conduction branches are favorable for exploring novel electronic functionalities for RF applications, such as ambipolar frequency multipliers and ambipolar mixers that can utilize the symmetrical properties of the device to either simplify the circuitries required for realizing these functions or to enhance its performance. BP electronic modulators, frequency multipliers, and inverters have been demonstrated by Zhu et al. on flexible substrates, highlighting the potential of BP-based devices for high-frequency thin-film electronic applications.[74] Recently, an ambipolar charge trapping memory device based on BP has been reported by Tian et al. that features dynamically reconfigurable and polarity-reversible memory behaviors.[76] The device can offer adaptable memory characteristics as a useful building block for constructing dynamically reconfigurable circuits and data-adaptive energy-efficient memory.

The anisotropic electronic properties of black phosphorus can also lead to new device concepts for the emerging field of neuromorphic electronics. The connection strengths of the biological synapses vary significantly in neural networks, which enhance the diverse functionalities of the brain. Achieving such heterogeneity in electronic synapses is useful for developing artificial neural networks that can attain a higher level of complexity and functionality. The first black phosphorus based synaptic device demonstrated shows intrinsically heterogeneous synaptic characteristics deriving from its anisotropic transport properties.[76] Furthermore, the device takes advantage of the native oxide of BP, i.e., phosphorus oxide, which utilizes the charge trapping layer that enables the synaptic characteristics through the trapping and de-trapping of electrons as electrical pulses are applied at the gate electrode. The different synaptic characteristics for devices built along the x and y-directions of the BP crystal are attributed to the different trapped charge induced scattering in the carrier mobility along different BP crystal directions. A compact network was also demonstrated using a radial shape BP synaptic device layout that mimics a heterogeneous one-axon-multisynapse connection in biological neural network. Such devices and network blocks can help enhance the functionalities of electronic synaptic network. While these early BP-based circuits are quite different from actual neurons, they provide an interesting material system for exploring basic device and circuit concepts.

4. Stable Anisotropic Electronic and Quasiparticle Properties

Permanent alteration of the surface of BP due to degradation affects its fundamental physical properties such as of topologically protected surface states, surface polaritons, and excitons. Robust topological insulators such as Bi_2Se_3 are sensitive to atmospheric exposure induced n-doping of the surface, which compromises the relative contribution of topological surface states to conductivity.[77] Topological states in unprotected BP can also be expected to suffer similar unintentional doping. More severe chemical alteration of the surface due to atmospheric exposure will significantly suppress surface states, potentially making the surface of BP more insulting than the bulk. Surface oxidation can also result in strong modification of BP band structure[78] though the oxidized layer may stabilize the surface by acting as a protective capping layer against further degradation. However, an oxide surface can act as an unwanted source of surface and interface traps and charged states, which is detrimental to the fabrication of multilayer devices.[39,52] The surface oxidation effect is analogous to a similar oxidation process that has been observed in and hence been a major cause for concern in III–V metal oxide semiconductor field effect transistor. Experimental investigations of physical properties of BP have been performed both under ambient conditions with or without protected BP and in vacuum providing valuable insight into this material's fundamental intrinsic properties.

The highly anisotropic band dispersion around the band gap results in a corresponding highly anisotropic effective mass and as a result anisotropic electric conductance.[79,80]

From first-principles simulations, Fei and Yang[79] have shown that the unique anisotropic conductance can be manipulated further using strain. Mishchenko et al. have also measured anisotropy in electronic properties of ≈10 nm thick BP flakes.[81] Optically Mao et al. reported (**Figure 6**a–d) anisotropy of few-layer BP in the visible regime simply by using polarized optical microscopy.[82] Ling et al. also took advantage of this anisotropy to identify the crystal orientation of BP demonstrating a simple noninvasive method for identification of these crystal axes.[83]

Anisotropic excitons, phonons, and plasmons in BP play a unique role in modifying its physical properties. Employing polarization-sensitive photoluminesce experiments, Wang et al. revealed highly anisotropic strongly bound excitons in monolayer BP (Figure 6e).[84] Anisotropy is a distinguishing feature in BP that can open numerous practical applications. Selective excitonic emission can lead to opportunities for manipulation of light polarization that is unavailable in other 2D materials. However, under high excitation conditions, exciton–exciton annihilation can limit injection density reducing quantum yield.[85] Anisotropic thermal conductivity due to phonon dispersion was first reported by Luo et al.[86] Phonon modes can be tuned by application of strain.[87] Strong polarization and nonlinear temperature dependence as well as the existence of anisotropic edge phonon modes of BP have all been explored.[88–91] Due to anisotropy, polaritons propagating in BP can manipulated. Nemilentsau et al. proposed highly directional propagating hyperbolic plasmons via doping anisotropic BP, which can offer unprecedented control of directional plasmons that can be tuned on the spot.[92] Ultrathin BP is also predicted to host hyperbolic plasmons with nonlocality induced topological transitions and electrically tunable plasmon modes in bilayer BP.[93,94] The experimental observation of a hybrid polariton waves made of surface plasmon modes in BP and phonon polariton on SiO_2 substrate was also reported recently.[95]

BP's small band gap combined with its anisotropy makes it a candidate to observe exotic anisotropic surface states.[96] Recently Fei et al. proposed that bulk BP can become a topological semimetal via uniaxial structural deformation, which inverts the band gap.[97] The existence of Dirac cones with anisotropic Fermi velocities in BP means that both massless

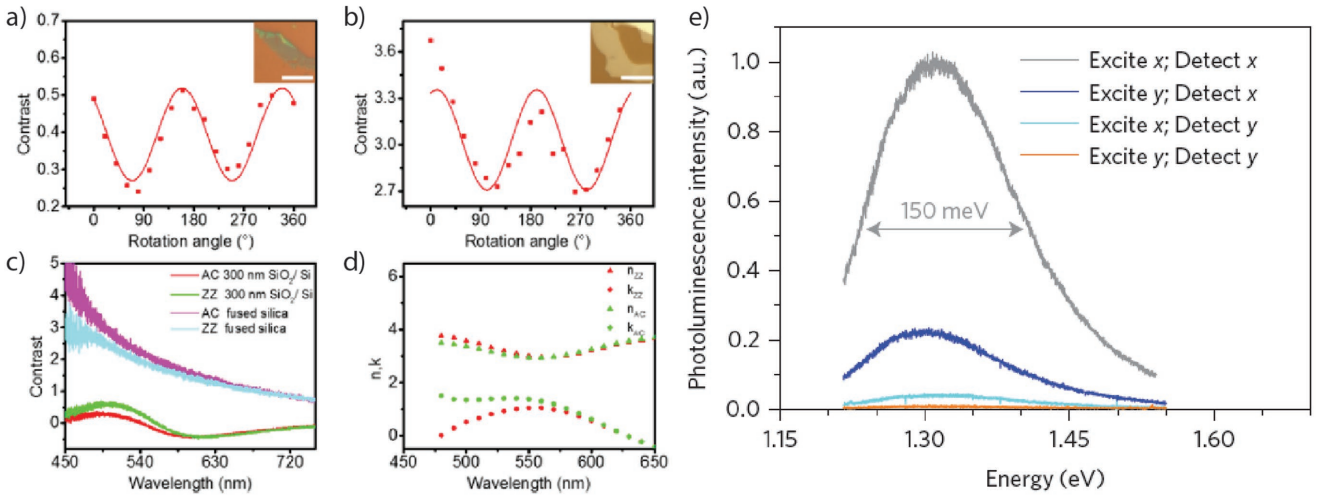

Figure 6. Simulated and measured anisotropic optical contrast and refractive indices for few-layer BP on 300 nm SiO_2/Si and fused silica substrate. Angle-dependent optical contrast of (a): a) the 5 nm BP samples on SiO_2/Si and b) fused silica under parallel polarizations. The wavelength of the incident light is 480 nm. c) Optical contrast spectra along AC and ZZ crystalline direction of 5 nm thick BP on SiO_2/Si and fused silica substrates, respectively. d) Measured refractive indices for 5 nm thick BP along AC and ZZ crystalline directions. The solid triangles and dots are the real and imaginary parts of the refractive indices, respectively. Reproduced with permission.[82] Copyright 2016, American Chemical Society. Exciton photoluminescence with large in-plane anisotropy. e) Polarization-resolved photoluminescence spectra, revealing the excitonic nature of emission from the monolayer black phosphorus. The excitation 532 nm laser is linearly polarized along either *x* (grey curves) or *y* (blue curves) directions. On the detection side, a halfwave plate and linear polarizer selects *x* or *y*-polarized components of the emitted light, leading to a total of four different combinations as shown. Reproduced with permission.[84] Copyright 2015, Nature Publishing Group.

and massive carriers can simultaneously be present in the same material. This phenomenon has been experimentally observed by Xiang et al. on single crystal BP samples.[98] Liu et al. have proposed active tuning of anisotropic topological behavior in few-layer BP.[99] Despite its large band gap, application of external electric field can induce transition from normal insulator to a topological insulator in BP. Kim et al. have observed similar electric field modulated Dirac semimetal topological phase in BP as a result of potassium doping.[100] Graphene retains a linear (or "conical") dispersion relation at low energies. In contrast BP can form 1D or 2D Dirac cones that display tunable anisotropic dispersion. The ability to tune the band gap of BP using pressure[37,97,101] or applying an external field[99,100,102] for the generation of anisotropic exotic electronic states is promising for novel optoelectronic applications. For more details on anisotropy in BP, we direct the readers to refs. [1], [2], [7], and [9].

5. Conclusion and Perspectives

The long-term stability of BP appears to be reaching a level of certainty based on various aging studies of encapsulated films. ALD deposited metal oxides, fluoropolymers, and hydrophobic thin films all provide a measure of air stability with varying degrees of effectiveness. Double layers of ALD with high-*k* oxides and fluoropolymer provide a near-optimum BP device structure with high electrical performance and over a year long air stability. Passivation layers using vdW materials, like (*h*BN or graphite), and hybrid layers combining vdW materials with 3D inorganic or organic materials are also very promising particularly for monolayer BP. Coatings that utilize a 3D material with dangling bonds will introduce surface charged states and impurities at the interface with BP resulting in unintentional doping, charge scattering, and changes in the band structure. By using a vdW layer, an atomically abrupt and clean interface with BP can be formed, which can preserve intrinsic properties. In the hybrid structure, an encapsulation material with superior permeability properties along with a thin vdW layer can be used together to isolate and preserve BP. More longer term studies that span years or accelerated studies are, however, still required to ascertain the effectiveness of these passivation techniques for potential nanoelectronics applications. Recent bias-stress and temperature-stress testing on working BP transistor devices have shown reliable performance with only modest drift in the performance metrics such as threshold voltage. Some devices have also shown what is known as "positive aging," where there is slight improvement in electrical performance over time. "Positive aging" might arise from slow annealing of traps and defects or desorption of moisture that may have been trapped shortly before or during the process of encapsulation.[103]

In addition, phosphorene, the monolayer of BP, is far more air sensitive and difficult to prepare and/or integrate onto device structures. Therefore, there have been relatively few air-stability studies[104] in working devices. As such, future studies are warranted for this monolayer of BP, which offers the highest direct band gap and potentially the most attractive alternative for photovoltaic and low-power transistor devices. Recent synthesis progress has revealed that the growth of 2D phosphorus is achievable on metal surfaces by MBE. Therefore, it is imperative to develop transfer and air-stability schemes to expedite the integration of this large-scale synthetic monolayer onto device platforms for diverse studies and applications.

Significant progress is being made in understanding fundamental physical properties of single and multilayer BP. Fabrication of high-quality and stable samples enabled by various passivation techniques will facilitate these investigations. Understanding the effects of passivation on physical properties of BP samples will be important if practical performance is to be realized. The unique tunable band gap energy range and strong in-plane anisotropy of single and few-layer BP provide an exciting opportunity to explore dynamically controlled anisotropic surface polaritons (exciton, phonon, or plasmon) in this material. The possibility BP provides for manipulation of its band structure using external means such as electric fields opens the way to induce actively controlled quantum confined anisotropic topological states. Combining unique properties of BP with other vdW materials through top-down heterostructures fabrication and subsequent fine-tuning could open new opportunities for exciting fundamental science explorations.

Looking forward to the future, we see the need to push university-level synthesis methods for assembling heterostructures toward more scalable approaches for commercial applications. This will likely involve development of processes similar to those established for III–V semiconductors to epitaxially grow large area planar structures consisting of one to many thin-film materials. In this light, the recent synthesis progress demonstrating growth of 2D blue phosphorus on metal surfaces by MBE is a major first step forward. For BP passivation, capping layers can be directly grown in situ without having to expose surfaces to air. This could be achieved by incorporating multiple deposition systems like a phosphide MBE and an oxide ALD system. Alternatively, growth of heterostructures in a single MBE or chemical vapor deposition system can also be employed. With all the recent success in production of 2D heterostructures, it is likely that growing a 2D heterostructure with BP encapsulated between passivating 2D layers could also be achievable. Achieving such structures would allow for a relatively simple transfer to conventional planar device processing. However, we must also consider the limited thermal stability (<550 °C) of BP, which can turn out to be another challenge in itself considering many of the stable 2D layers require growth temperatures beyond the limit of BP stability. As such, approaches using ultra clean exfoliation or transfer practices in inert environments may be feasible in the near term as BP and 2D growth technology advance.

Acknowledgements

Y.A. acknowledges support provided by the National Science Foundation CAREER Grant No. 1553251. S.G. was supported by the Air Force Office of Scientific Research AFOSR Grant No. FA9559-16-1-0172. M.S. would like to thank the Air Force Office of Scientific Research for their support under Award No. FA9550-16RYCOR331. S.B.C. was supported by the Department of Energy Award No. DE-FG02-07ER46376 and N.P. was supported by the National Science Foundation NSF Award No. 1402906. H.W. acknowledges support from the National Science Foundation CAREER program (Grant No. ECCS-1653870) and the National Science Foundation EFRI 2-DARE program (Grant No. EFMA-1542815). D.A. acknowledges the support of a National Science Foundation EAGER grant. The authors acknowledge the assistance of Jiangbin Wu and Marquez Howard in preparing some of the figures.

Conflict of Interest

The authors declare no conflict of interest.

Keywords

2D materials, black phosphorus, degradation, layered materials, passivation

Received: August 20, 2017
Revised: December 29, 2017
Published online:

[1] X. Ling, H. Wang, S. Huang, F. Xia, M. S. Dresselhaus, *Proc. Natl. Acad. Sci. USA* **2015**, *112*, 4523.
[2] H. Liu, Y. Du, Y. Deng, P. D. Ye, *Chem. Soc. Rev.* **2015**, *44*, 2732.
[3] P. W. Bridgman, *J. Am. Chem. Soc.* **1916**, *38*, 609.
[4] E. Shoichi, A. Yuichi, T. Shin-ichi, N. Shin-ichiro, *Jpn. J. Appl. Phys.* **1982**, *21*, L482.
[5] M. Köpf, N. Eckstein, D. Pfister, C. Grotz, I. Krüger, M. Greiwe, T. Hansen, H. Kohlmann, T. Nilges, *J. Cryst. Growth* **2014**, *405*, 6.
[6] M. Batmunkh, M. Bat-Erdene, J. G. Shapter, *Adv. Mater.* **2016**, *28*, 8586.
[7] L. Kou, C. Chen, S. C. Smith, *J. Phys. Chem. Lett.* **2015**, *6*, 2794.
[8] A. Castellanos-Gomez, *J. Phys. Chem. Lett.* **2015**, *6*, 4280.
[9] V. Eswaraiah, Q. Zeng, Y. Long, Z. Liu, *Small* **2016**, *12*, 3480.
[10] S. Huang, X. Ling, *Small* **2017**, *13*, 1700823.
[11] Z. Yang, J. Hao, S. Yuan, S. Lin, H. M. Yau, J. Dai, S. P. Lau, *Adv. Mater.* **2015**, *27*, 3748.
[12] L. Xuesong, D. Bingchen, W. Xiaomu, C. Sizhe, V. Michelle, K. Shun-ichiro, P. Grace, L. Minjoo Larry, C. Judy, W. Han, X. Fengnian, *2D Mater.* **2015**, *2*, 031002.
[13] C. Gu, S. Zhao, J. L. Zhang, S. Sun, K. Yuan, Z. Hu, C. Han, Z. Ma, L. Wang, F. Huo, W. Huang, Z. Li, W. Chen, *ACS Nano* **2017**, *11*, 4943.
[14] R. Schuster, J. Trinckauf, C. Habenicht, M. Knupfer, B. Buchner, *Phys. Rev. Lett.* **2015**, *115*, 026404.
[15] J. A. Schuller, S. Karaveli, T. Schiros, K. He, S. Yang, I. Kymissis, J. Shan, R. Zia, *Nat. Nanotechnol.* **2013**, *8*, 271.
[16] A. R. Klots, A. K. M. Newaz, B. Wang, D. Prasai, H. Krzyzanowska, J. Lin, D. Caudel, N. J. Ghimire, J. Yan, B. L. Ivanov, K. A. Velizhanin, A. Burger, D. G. Mandrus, N. H. Tolk, S. T. Pantelides, K. I. Bolotin, *Sci. Rep.* **2014**, *4*, 6608.
[17] Z. Ye, T. Cao, K. O'Brien, H. Zhu, X. Yin, Y. Wang, S. G. Louie, X. Zhang, *Nature* **2014**, *513*, 214.
[18] K. F. Mak, K. He, C. Lee, G. H. Lee, J. Hone, T. F. Heinz, J. Shan, *Nat. Mater.* **2013**, *12*, 207.
[19] J. S. Ross, S. Wu, H. Yu, N. J. Ghimire, A. M. Jones, G. Aivazian, J. Yan, D. G. Mandrus, D. Xiao, W. Yao, X. Xu, *Nat. Commun.* **2013**, *4*, 1474.
[20] A. M. Jones, H. Y. Yu, N. J. Ghimire, S. F. Wu, G. Aivazian, J. S. Ross, B. Zhao, J. Q. Yan, D. G. Mandrus, D. Xiao, W. Yao, X. D. Xu, *Nat. Nanotechnol.* **2013**, *8*, 634.
[21] H. Liu, A. T. Neal, Z. Zhu, Z. Luo, X. Xu, D. Tománek, P. D. Ye, *ACS Nano* **2014**, *8*, 4033.
[22] B. Deng, V. Tran, Y. Xie, H. Jiang, C. Li, Q. Guo, X. Wang, H. Tian, S. J. Koester, H. Wang, J. J. Cha, Q. Xia, L. Yang, F. Xia, *Nat. Commun.* **2017**, *8*, 14474.
[23] F. Liu, Q. Shi, J. Wang, H. Guo, *Appl. Phys. Lett.* **2015**, *107*, 203501.
[24] G. Long, D. Maryenko, J. Shen, S. Xu, J. Hou, Z. Wu, W. K. Wong, T. Han, J. Lin, Y. Cai, R. Lortz, N. Wang, *Nano Lett.* **2016**, *16*, 7768.

[25] L. Li, Y. Yu, G. J. Ye, Q. Ge, X. Ou, H. Wu, D. Feng, X. H. Chen, Y. Zhang, *Nat. Nanotechnol.* **2014**, *9*, 372.
[26] T. Low, R. Roldan, H. Wang, F. Xia, P. Avouris, L. Martin Moreno, F. Guinea, *Phys. Rev. Lett.* **2014**, *113*, 106802.
[27] J. Pei, X. Gai, J. Yang, X. Wang, Z. Yu, D.-Y. Choi, B. Luther-Davies, Y. Lu, *Nat. Commun.* **2016**, *7*, 10450.
[28] C. R. Ryder, J. D. Wood, S. A. Wells, M. C. Hersam, *ACS Nano* **2016**, *10*, 3900.
[29] S. Gamage, Z. Li, V. S. Yakovlev, C. Lewis, H. Wang, S. B. Cronin, Y. Abate, *Adv. Mater. Interfaces* **2016**, *3*, 1600121.
[30] J. D. Wood, S. A. Wells, D. Jariwala, K. S. Chen, E. Cho, V. K. Sangwan, X. L. Liu, L. J. Lauhon, T. J. Marks, M. C. Hersam, *Nano Lett.* **2014**, *14*, 6964.
[31] S. L. Yau, T. P. Moffat, A. J. Bard, Z. Zhang, M. M. Lerner, *Chem. Phys. Lett.* **1992**, *198*, 383.
[32] A. Castellanos-Gomez, L. Vicarelli, E. Prada, J. O. Island, K. L. Narasimha-Acharya, S. I. Blanter, D. J. Groenendijk, M. Buscema, G. A. Steele, J. V. Alvarez, H. W. Zandbergen, J. J. Palacios, H. S. J. van der Zant, *2D Mater.* **2014**, *1*, 025001.
[33] W. Sumeet, S. Ylias, A. Taimur, R. F. Matthew, R. Rajesh, A. Aram, K. B. Suresh, S. Sharath, B. Madhu, B. Vipul, B. Sivacarendran, *2D Mater.* **2017**, *4*, 015025.
[34] F. Alsaffar, S. Alodan, A. Alrasheed, A. Alhussain, N. Alrubaiq, A. Abbas, M. R. Amer, *Sci Rep.* **2017**, *7*, 44540.
[35] A. Favron, E. Gaufres, F. Fossard, A.-L. Phaneuf-Lheureux, N. Y. W. Tang, P. L. Levesque, A. Loiseau, R. Leonelli, S. Francoeur, R. Martel, *Nat. Mater.* **2015**, *14*, 826.
[36] G. Abellán, S. Wild, V. Lloret, N. Scheuschner, R. Gillen, U. Mundloch, J. Maultzsch, M. Varela, F. Hauke, A. Hirsch, *J. Am. Chem. Soc.* **2017**, *139*, 10432.
[37] A. S. Rodin, A. Carvalho, A. H. Castro Neto, *Phys. Rev. Lett.* **2014**, *112*, 176801.
[38] W. Lou, Y. Z. Dmitry, A. M. Cory, D. Yuchen, Y. Lingming, W. Yanqing, D. Y. Peide, *Nanotechnology* **2016**, *27*, 434002.
[39] Q. Zhou, Q. Chen, Y. Tong, J. Wang, *Angew. Chem., Int. Ed.* **2016**, *55*, 11437.
[40] R. A. Doganov, E. C. T. O'Farrell, S. P. Koenig, Y. Yeo, A. Ziletti, A. Carvalho, D. K. Campbell, D. F. Coker, K. Watanabe, T. Taniguchi, A. H. Castro Neto, B. Öezyilmaz, *Nat. Commun.* **2015**, *6*, 6647.
[41] J. O. Island, G. A. Steele, H. S. J. van der Zant, A. Castellanos-Gomez, *2D Mater.* **2015**, *2*, 011002.
[42] M. Serrano-Ruiz, M. Caporali, A. Ienco, V. Piazza, S. Heun, M. Peruzzini, *Adv. Mater. Interfaces* **2016**, *3*, 1500441.
[43] A. Ziletti, A. Carvalho, D. K. Campbell, D. F. Coker, A. H. Castro Neto, *Phys. Rev. Lett.* **2015**, *114*, 046801.
[44] W. Gaoxue, J. S. William, P. Ravindra, P. K. Shashi, *2D Mater.* **2016**, *3*, 025011.
[45] Y. Huang, J. Qiao, K. He, S. Bliznakov, E. Sutter, X. Chen, D. Luo, F. Meng, D. Su, J. Decker, W. Ji, R. S. Ruoff, P. Sutter, *Chem. Mater.* **2016**, *28*, 8330.
[46] C. R. Ryder, J. D. Wood, S. A. Wells, Y. Yang, D. Jariwala, T. J. Marks, G. C. Schatz, M. C. Hersam, *Nat. Chem.* **2016**, *8*, 597.
[47] Y. Zhao, H. Wang, H. Huang, Q. Xiao, Y. Xu, Z. Guo, H. Xie, J. Shao, Z. Sun, W. Han, X.-F. Yu, P. Li, P. K. Chu, *Angew. Chem., Int. Ed.* **2016**, *55*, 5003.
[48] Q. Li, Q. Zhou, X. Niu, Y. Zhao, Q. Chen, J. Wang, *J. Phys. Chem. Lett.* **2016**, *7*, 4540.
[49] G. Abellán, V. Lloret, U. Mundloch, M. Marcia, C. Neiss, A. Görling, M. Varela, F. Hauke, A. Hirsch, *Angew. Chem., Int. Ed.* **2016**, *55*, 14557.
[50] X. Chen, Y. Wu, Z. Wu, Y. Han, S. Xu, L. Wang, W. Ye, T. Han, Y. He, Y. Cai, N. Wang, *Nat. Commun.* **2015**, *6*, 7315.
[51] S. Gamage, A. Fali, N. Aghamiri, L. Yang, P. D. Ye, Y. Abate, *Nanotechnology* **2017**, *28*, 265201.
[52] M. T. Edmonds, A. Tadich, A. Carvalho, A. Ziletti, K. M. O'Donnell, S. P. Koenig, D. F. Coker, B. Özyilmaz, A. H. C. Neto, M. S. Fuhrer, *ACS Appl. Mater. Interfaces* **2015**, *7*, 14557.
[53] P. Li, D. Zhang, J. Liu, H. Chang, Y. e. Sun, N. Yin, *ACS Appl. Mater. Interfaces* **2015**, *7*, 24396.
[54] Y. Cao, A. Mishchenko, G. L. Yu, E. Khestanova, A. P. Rooney, E. Prestat, A. V. Kretinin, P. Blake, M. B. Shalom, C. Woods, J. Chapman, G. Balakrishnan, I. V. Grigorieva, K. S. Novoselov, B. A. Piot, M. Potemski, K. Watanabe, T. Taniguchi, S. J. Haigh, A. K. Geim, R. V. Gorbachev, *Nano Lett.* **2015**, *15*, 4914.
[55] J. S. Kim, Y. Liu, W. Zhu, S. Kim, D. Wu, L. Tao, A. Dodabalapur, K. Lai, D. Akinwande, *Sci. Rep.* **2015**, *5*, 8989.
[56] D. Hanlon, C. Backes, E. Doherty, C. S. Cucinotta, N. C. Berner, C. Boland, K. Lee, A. Harvey, P. Lynch, Z. Gholamvand, S. Zhang, K. Wang, G. Moynihan, A. Pokle, Q. M. Ramasse, N. McEvoy, W. J. Blau, J. Wang, G. Abellan, F. Hauke, A. Hirsch, S. Sanvito, D. D. O'Regan, G. S. Duesberg, V. Nicolosi, J. N. Coleman, *Nat. Commun.* **2015**, *6*, 8563.
[57] S. Koenig, R. A. Doganov, H. Schmidt, A. H. Neto, B. Ozyilmaz, *Appl. Phys. Lett.* **2014**, *104*, 103106.
[58] H. Du, X. Lin, Z. Xu, D. Chu, *J. Mater. Chem. C* **2015**, *3*, 8760.
[59] R. Pal, R. K. Bhan, K. C. Chhabra, O. P. Agnihotri, *Semicond. Sci. Technol.* **1996**, *11*, 231.
[60] R. Babar, M. Kabir, *J. Phys. Chem. C* **2016**, *120*, 14991.
[61] R. A. D. S. P. Koenig, L. Seixas, A. Carvalho, J. Y. Tan, K. Watanabe, T. Taniguchi, N. Yakovlev, A. H. C. Neto, B. Özyilmaz, *Nano Lett.* **2016**, *16*, 7.
[62] Z. Guo, S. Chen, Z. Wang, Z. Yang, F. Liu, Y. Xu, J. Wang, Y. Yi, H. Zhang, L. Liao, P. K. Chu, X.-F. Yu, *Adv. Mater.* **2017**, *29*, 1703811.
[63] Y. Jing, Q. Tang, P. He, Z. Zhou, P. W. Shen, *Nanotechnology* **2015**, *26*, 095201.
[64] J. Kang, J. D. Wood, S. A. Wells, J.-H. Lee, X. Liu, K.-S. Chen, M. C. Hersam, *ACS Nano* **2015**, *9*, 3596.
[65] A. Avsar, I. J. Vera-Marun, J. Y. Tan, K. Watanabe, T. Taniguchi, A. H. Castro Neto, B. Özyilmaz, *ACS Nano* **2015**, *9*, 4138.
[66] F. Xia, H. Wang, Y. Jia, *Nat. Commun.* **2014**, *5*, 4458.
[67] L. M. Yang, G. Qiu, M. W. Si, A. R. Charnas, C. A. Milligan, D. Y. Zemlyanov, H. Zhou, Y. C. Du, Y. M. Lin, W. Tsai, Q. Paduano, M. Snure, P. D. Ye, presented at *2016 IEEE Int. Electron Devices Meeting (IEDM)*, San Francisco, CA, December **2016**.
[68] Y. Zhao, Q. Zhou, Q. Li, X. Yao, J. Wang, *Adv. Mater.* **2017**, *29*, 1603990.
[69] W. Bensong, Y. Bingchao, W. Yue, Z. Junying, Z. Zhongming, L. Zhongyuan, W. Wenhong, *Nanotechnology* **2015**, *26*, 435702.
[70] J. Kim, S. K. Baek, K. S. Kim, Y. J. Chang, E. J. Choi, *Curr. Appl. Phys.* **2016**, *16*, 165.
[71] H.-Y. Chang, S. Yang, J. Lee, L. Tao, W.-S. Hwang, D. Jena, N. Lu, D. Akinwande, *ACS Nano* **2013**, *7*, 5446.
[72] S. Das, R. Gulotty, A. V. Sumant, A. Roelofs, *Nano Lett.* **2014**, *14*, 2861.
[73] D. B. Mitzi, L. L. Kosbar, C. E. Murray, M. Copel, A. Afzali, *Nature* **2004**, *428*, 299.
[74] W. Zhu, M. N. Yogeesh, S. Yang, S. H. Aldave, J. S. Kim, S. Soude, L. Tao, N. Lu, D. Akinwande, *Nano Lett.* **2015**, *15*, 1883.
[75] H. Wang, X. Wang, F. Xia, L. Wang, H. Jiang, Q. Xia, M. L. Chin, M. Dubey, S.-j. Han, *Nano Lett.* **2014**, *14*, 6424.
[76] H. Tian, Q. Guo, Y. Xie, H. Zhao, C. Li, J. J. Cha, F. Xia, H. Wang, *Adv. Mater.* **2016**, *28*, 4991.
[77] D. Kong, J. J. Cha, K. Lai, H. Peng, J. G. Analytis, S. Meister, Y. Chen, H.-J. Zhang, I. R. Fisher, Z.-X. Shen, Y. Cui, *ACS Nano* **2011**, *5*, 4698.
[78] J. Lu, J. Wu, A. Carvalho, A. Ziletti, H. Liu, J. Tan, Y. Chen, A. H. Castro Neto, B. Özyilmaz, C. H. Sow, *ACS Nano* **2015**, *9*, 10411.

[79] R. Fei, L. Yang, *Nano Lett.* **2014**, *14*, 2884.
[80] J. Qiao, X. Kong, Z.-X. Hu, F. Yang, W. Ji, *Nat. Commun.* **2014**, *5*, 4475.
[81] A. Mishchenko, Y. Cao, G. L. Yu, C. R. Woods, R. V. Gorbachev, K. S. Novoselov, A. K. Geim, L. S. Levitov, *Nano Lett.* **2015**, *15*, 6991.
[82] N. Mao, J. Tang, L. Xie, J. Wu, B. Han, J. Lin, S. Deng, W. Ji, H. Xu, K. Liu, L. Tong, J. Zhang, *J. Am. Chem. Soc.* **2016**, *138*, 300.
[83] X. Ling, S. Huang, E. H. Hasdeo, L. Liang, W. M. Parkin, Y. Tatsumi, A. R. T. Nugraha, A. A. Puretzky, P. M. Das, B. G. Sumpter, D. B. Geohegan, J. Kong, R. Saito, M. Drndic, V. Meunier, M. S. Dresselhaus, *Nano Lett.* **2016**, *16*, 2260.
[84] X. Wang, A. M. Jones, K. L. Seyler, T. Vy, Y. Jia, H. Zhao, H. Wang, L. Yang, X. Xu, F. Xia, *Nat. Nanotechnol.* **2015**, *10*, 517.
[85] A. Surrente, A. A. Mitioglu, K. Galkowski, L. Klopotowski, W. Tabis, B. Vignolle, D. K. Maude, P. Plochocka, *Phys. Rev. B* **2016**, *94*, 075425.
[86] Z. Luo, J. Maassen, Y. Deng, Y. Du, R. P. Garrelts, M. S. Lundstrom, P. D. Ye, X. Xu, *Nat. Commun.* **2015**, *6*, 8572.
[87] Y. Wang, C. Cong, R. Fei, W. Yang, Y. Chen, B. Cao, L. Yang, T. Yu, *Nano Res.* **2015**, *8*, 3944.
[88] J. Jin-Wu, W. Bing-Shen, S. P. Harold, *J. Phys.: Condens. Matter* **2016**, *28*, 165401.
[89] M. Snure, S. Vangala, D. Walker, *Opt. Mater. Express* **2016**, *6*, 1751.
[90] H. B. Ribeiro, C. E. P. Villegas, D. A. Bahamon, D. Muraca, A. H. Castro Neto, E. A. T. de Souza, A. R. Rocha, M. A. Pimenta, C. J. S. de Matos, *Nat. Commun.* **2016**, *7*, 12191.
[91] A. Łapińska, A. Taube, J. Judek, M. Zdrojek, *J. Phys. Chem. C* **2016**, *120*, 5265.
[92] A. Nemilentsau, T. Low, G. Hanson, *Phys. Rev. Lett.* **2016**, *116*, 066804.
[93] D. Correas-Serrano, J. S. Gomez-Diaz, A. A. Melcon, A. Andrea, *J. Opt.* **2016**, *18*, 104006.
[94] F. Jin, R. Roldán, M. I. Katsnelson, S. Yuan, *Phys. Rev. B* **2015**, *92*, 115440.
[95] M. A. Huber, F. Mooshammer, M. Plankl, L. Viti, F. Sandner, L. Z. Kastner, T. Frank, J. Fabian, M. S. Vitiello, T. L. Cocker, R. Huber, *Nat. Nanotechnol.* **2016**, *12*, 207.
[96] Y. Abate, S. Gamage, Z. Li, V. Babicheva, M. H. Javani, H. Wang, S. B. Cronin, M. I. Stockman, *Light: Sci. Appl.* **2016**, *5*, e16162.
[97] R. Fei, V. Tran, L. Yang, *Phys. Rev. B* **2015**, *91*, 195319.
[98] Z. J. Xiang, G. J. Ye, C. Shang, B. Lei, N. Z. Wang, K. S. Yang, D. Y. Liu, F. B. Meng, X. G. Luo, L. J. Zou, Z. Sun, Y. Zhang, X. H. Chen, *Phys. Rev. Lett.* **2015**, *115*, 186403.
[99] Q. Liu, X. Zhang, L. B. Abdalla, A. Fazzio, A. Zunger, *Nano Lett.* **2015**, *15*, 1222.
[100] J. Kim, S. S. Baik, S. H. Ryu, Y. Sohn, S. Park, B.-G. Park, J. Denlinger, Y. Yi, H. J. Choi, K. S. Kim, *Science* **2015**, *349*, 723.
[101] E. Taghizadeh Sisakht, F. Fazileh, M. H. Zare, M. Zarenia, F. M. Peeters, *Phys. Rev. B* **2016**, *94*, 085417.
[102] E. Motohiko, *New J. Phys.* **2014**, *16*, 115004.
[103] Y. Y. Illarionov, M. Waltl, G. Rzepa, T. Knobloch, J. S. Kim, D. Akinwande, T. Grasser, *npj 2D Mater. Appl.* **2017**, *1*, 23.
[104] Y. Y. Illarionov, M. Waltl, G. Rzepa, J.-S. Kim, S. Kim, A. Dodabalapur, D. Akinwande, T. Grasser, *ACS Nano* **2016**, *10*, 9543.